Bulk viscosity of multiparticle collision dynamics fluids

Mario Theers* and Roland G. Winkler†
Theoretical Soft Matter and Biophysics, Institute for Advanced Simulation and Institute of Complex Systems, Forschungszentrum Jülich, D-52425 Jülich, Germany
(Received 18 February 2015; published 26 March 2015)

We determine the viscosity parameters of the multiparticle collision dynamics (MPC) approach, a particle-based mesoscale hydrodynamic simulation method for fluids. We perform analytical calculations and verify our results by simulations. The stochastic rotation dynamics and the Andersen thermostat variant of MPC are considered, both with and without angular momentum conservation. As an important result, we find a nonzero bulk viscosity for every MPC version. The explicit calculation shows that the bulk viscosity is determined solely by the collisional interactions of MPC.

DOI: 10.1103/PhysRevE.91.033309 PACS number(s): 47.11.−j, 02.70.Ns, 66.20.−d

I. INTRODUCTION

During the past few decades, various mesoscale hydrodynamic simulation techniques have been developed and have been applied to study soft matter systems. Prominent examples are the lattice-Boltzmann (LB) technique [1–3], dissipative particle dynamics (DPD) [4,5], and multiparticle collision dynamics (MPC) [6–9]. Common to these approaches is a simplified, coarse-grained description of the fluid degrees of freedom while maintaining the essential microscopic physics on the length scales of interest. As a consequence, this leads to particular equations of state, in the simplest case that of an ideal gas, as is true for LB and MPC. The question is then to what extent other quantities, e.g., transport coefficients, are similar to those of an ideal gas. Here, of particular interest is the bulk viscosity, which is considered to be zero for monatomic gases [10–12]. However, calculations yield a nonzero bulk viscosity for LB [3]. As far as MPC is concerned, zero [11,13,14] and nonzero [11,15] bulk viscosity values have been reported.

Multiparticle collision dynamics is a particle-based hydrodynamic simulation method, which incorporates thermal fluctuations, provides hydrodynamic correlations, and is easily coupled with other simulation techniques, such as molecular-dynamics simulations for embedded particles [8,9]. MPC proceeds in a ballistic streaming step and a collision step. Collisions occur at fixed discrete time intervals and establish a local stochastic interaction between particles. Thereby, the particles are sorted into cells to define the multiparticle-collision environment. Various schemes for the collisional interaction have been proposed [6–9,16,17]. The original method, which employs rotation of relative velocities, is often denoted as stochastic-rotation dynamics (SRD) [6–9,16,17]. Other methods, adopting an Andersen-thermostat-like idea, denoted as MPC-AT, use Gaussian-distributed random numbers for the relative velocities [16,17]. In the simplest version, angular momentum is not conserved in a collision. However, angular-momentum-conserving extensions have been introduced for both the stochastic rotation version of MPC (MPC-SRD+a) and the Andersen variant (MPC-AT+a) [17,18]. The MPC method has successfully been applied to a broad range of soft matter systems ranging from equilibrium colloid [6,8,9,19–27] and polymer [8,9,28–30] solutions and, more importantly, nonequilibrium systems such as colloids [16,31–35], polymers [29,36–45], vesicles [46], and cells [47,48] in flow fields, colloids in viscoelastic fluids [49–51], to self-propelled spheres [52–54], rods [8,55], and other microswimmers [18,56–59]. Moreover, extensions have been proposed for fluids with nonideal equations of state [60] and mixtures [61].

The hydrodynamic properties of the MPC fluid manifest themselves in the stress tensor, which, for an isotropic system, has three viscosity parameters in general [62]. For MPC, the shear viscosity has been analyzed theoretically and numerically [7–9,11,15,63–66], and good agreement has been found between the theoretical expression and the numerically obtained values for a three-dimensional nonangular-momentum-conserving SRD fluid (MPC-SRD−a) [67]. However, little is known about the bulk viscosity, although the simulations of Ref. [14] suggest a zero bulk viscosity for two-dimensional MPC fluids. Yet a recent study of circular Couette flow between a slip and a no-slip cylinder suggests a nonzero bulk viscosity for a MPC-SRD−a fluid [68].

In this article, we determine all relevant viscosity parameters of MPC fluids, and we demonstrate that the bulk viscosity is finite for both angular-momentum-conserving and nonangular-momentum-conserving MPC variants. Moreover, we derive an analytical expression for the bulk viscosity and confirm it by simulations.

The outline of the paper is as follows. In Sec. II, we introduce the MPC simulation method. The form of the stress tensor is discussed in Sec. III, and the viscosity parameters are determined analytically in Sec. IV. Simulation results are presented in Sec. V. Finally, Sec. VI summarizes our findings.

II. MULTIPARTICLE COLLISION DYNAMICS

A. Algorithm

The MPC fluid consists of N point particles with mass m, continuous positions $\boldsymbol{r}_i$, and velocities $\boldsymbol{v}_i$, which undergo streaming and subsequent collision steps. In the streaming step, the particles move ballistically during the time interval h, denoted as collision time, and their positions are updated

*m.theers@fz-juelich.de
†r.winkler@fz-juelich.de

according to

$$\boldsymbol{r}_i(t+h) = \boldsymbol{r}_i(t) + h\boldsymbol{v}_i(t). \tag{1}$$

In the collision step, the rectangular cuboid fluid volume V of dimensions $L_x \times L_y \times L_z$ is divided into cubic cells of length a to define the multiparticle collision environment. Particles sharing a cell exchange momenta in a stochastic process, whereby the total linear momentum is conserved. The velocity $\boldsymbol{v}_i(t+h)$ of particle i after collision is given by

$$\boldsymbol{v}_i(t+h) = \boldsymbol{v}_{\text{c.m.}}(t) + \mathcal{C}[\boldsymbol{v}_{ic}(t)]. \tag{2}$$

Here, $\boldsymbol{v}_{\text{c.m.}} = (1/N_c)\sum_{i=1}^{N_c} \boldsymbol{v}_i$ is the center-of-mass velocity, $\boldsymbol{v}_{ic} = \boldsymbol{v}_i - \boldsymbol{v}_{\text{c.m.}}$ is the particle's relative velocity with respect to the center-of-mass velocity, N_c is the total number of particles in the cell, and $\mathcal{C}$ is the collision operator.

For MPC-SRD−a, the operator $\mathcal{C}$ is a rotation around a randomly oriented axis by the constant angle α, i.e.,

$$\mathcal{C}[\boldsymbol{v}_{ic}] = \mathbf{R}(\alpha)\boldsymbol{v}_{ic}. \tag{3}$$

The orientation of the rotation axis is chosen independently for every collision cell and at every step [6,8,9].

In MPC-AT−a, a velocity $\boldsymbol{v}_i^{\text{ran}}$ is chosen for each particle i with Gaussian-distributed Cartesian components of zero mean and variance k_BT/m [16], where k_B is Boltzmann's constant and T is the temperature. The collision operator is then defined as

$$\mathcal{C}[\boldsymbol{v}_{ic}] = \boldsymbol{v}_i^{\text{ran}} - \frac{1}{N_c}\sum_{j=1}^{N_c} \boldsymbol{v}_j^{\text{ran}}. \tag{4}$$

MPC-SRD and MPC-AT correspond to a microcanonical and a canonical ensemble, respectively. By means of a cell-level canonical thermostat [29], a canonical ensemble is obtained for MPC-SRD, if desired. Throughout this paper, we will exclusively work within the canonical ensemble, i.e., we will apply the Maxwell-Boltzmann scaling approach (MBS), described in Ref. [29], to control temperature on a collision-cell level.

To conserve angular momentum, in each cell a rigid body rotation of the fluid-particle velocities is performed, which yields the particle velocities after a collision [17],

$$\boldsymbol{v}_i(t+h) = \boldsymbol{v}_{\text{c.m.}}(t) + \mathcal{C}[\boldsymbol{v}_{ic}(t)] + \boldsymbol{\omega} \times \boldsymbol{r}_{ic}(t+h), \tag{5}$$

where the angular velocity $\boldsymbol{\omega}$ is

$$\boldsymbol{\omega} = m\mathbf{I}^{-1}\sum_{j=1}^{N_c} (\boldsymbol{r}_{jc}(t+h) \times \{\boldsymbol{v}_{jc}(t) - \mathcal{C}[\boldsymbol{v}_{jc}(t)]\}). \tag{6}$$

Here, $\mathbf{I}$ is the moment-of-inertia tensor of the respective particles in the center-of-mass reference frame at time $t+h$, $\boldsymbol{r}_{\text{c.m.}} = (1/N_c)\sum_{i=1}^{N_c} \boldsymbol{r}_i$ is the center-of-mass position, and $\boldsymbol{r}_{ic} = \boldsymbol{r}_i - \boldsymbol{r}_{\text{c.m.}}$. Equation (5) can only be applied to MPC-SRD if a thermostat is used, since energy conservation is violated by the rotation.

Partition of the system into collision cells leads to a violation of Galilean invariance. To reestablish Galilean invariance, a random shift of the collision-cell lattice is introduced at every collision step [63,69]. For practical reasons, we equivalently shift the particle positions during their sorting into collision cells, i.e., the positions for particle sorting are given by $\boldsymbol{r}_i + \boldsymbol{s}$, where the Cartesian components s_α ($\alpha \in \{x,y,z\}$) of the shift vector $\boldsymbol{s}$ are taken from a uniform distribution in the interval $[-a/2,a/2]$. Note that the shifted particle positions have to satisfy the boundary conditions.

We apply three-dimensional periodic boundary conditions for all simulations. Shear flow is implemented by Lees-Edwards boundary conditions [70].

B. Stress tensor

A virial expression for the stress tensor $\sigma_{\alpha\beta}$, $\sigma_{\alpha\beta}$ measures the internal forces per area in the α direction acting on a surface with normal vector in the β direction, for a MPC fluid has been derived in Ref. [66],

$$\sigma_{\alpha\beta}^i = -\frac{1}{V}\sum_{i=1}^{N} m[v_{i\alpha} - v_\alpha(\boldsymbol{r}_i)][v_{i\beta} - v_\beta(\boldsymbol{r}_i)] - \frac{1}{Vh}\sum_{i=1}^{N} \Delta p_{i\alpha}\Delta r_{i\beta}. \tag{7}$$

Here, $\boldsymbol{r}_i$ is the position of particle i in the primary box, i.e., the minimum image convention is applied [70], $v_\alpha(\boldsymbol{r}_i)$ is the mean velocity field at $\boldsymbol{r} = \boldsymbol{r}_i$ [66,71], $\Delta\boldsymbol{p}_i$ is the change of momentum of particle i due to the collision, and $\Delta\boldsymbol{r}_i = \boldsymbol{r}_i - \boldsymbol{r}_c$ is the position of particle i relative to the center of its cell $\boldsymbol{r}_c$. Originally, $r_{i\beta}$ instead of $\Delta r_{i\beta}$ appears in the second term of the stress tensor (7) [66], but $r_{i\beta}$ and $\Delta r_{i\beta}$ only differ by the constant vector $\boldsymbol{r}_c$ and $\sum_{i\in\text{cell}} \Delta p_{i\alpha} r_{c\beta} = 0$, since the total momentum change in a cell is zero. We denote the first and second term as the kinetic and collisional stress tensor, respectively, i.e., $\sigma_{\alpha\beta} = \sigma_{\alpha\beta}^k + \sigma_{\alpha\beta}^c$. At equilibrium, the average of the collisional stress tensor vanishes, because the momentum exchange and the particle position are independent. In the case of an applied shear flow along the x axis, the mean velocity field $v_\alpha(\boldsymbol{r}_i)$ is given by

$$v_x = \dot\gamma r_z, \quad v_y = v_z = 0, \tag{8}$$

where $\dot\gamma$ is the shear rate.

In the steady state, we can perform a time average as discussed in Ref. [66], which yields

$$\sigma_{xz} = \langle\sigma_{xz}^i\rangle = -\left\langle \frac{1}{V}\sum_{i=1}^{N} m v_{ix}v_{iz} + \frac{\dot\gamma h}{2V}\sum_{i=1}^{N} m v_{iz}^2 + \frac{1}{Vh}\sum_{i=1}^{N} \Delta p_{ix}\Delta r_{iz}\right\rangle_T, \tag{9}$$

where $\langle\cdots\rangle_T$ denotes the average over time steps [66]. The velocities $\boldsymbol{v}_i$ are taken before collision and in the primary box of the periodic system.

III. HYDRODYNAMICS

A. Continuum stress and Navier-Stokes equations

On large length and time scales, a MPC fluid is well described in terms of a continuous velocity field $\boldsymbol{v}(\boldsymbol{r},t)$ by the Navier-Stokes equations [6,8,11,15,18,72], which, in

linearized form, read

$$\frac{\partial}{\partial t}\delta\rho(\boldsymbol{r},t)+\rho_0\nabla\cdot\boldsymbol{v}(\boldsymbol{r},t)=0, \tag{10}$$

$$\rho_0\frac{\partial}{\partial t}\boldsymbol{v}(\boldsymbol{r},t)=\nabla\cdot\boldsymbol{\sigma}(\boldsymbol{r},t) \tag{11}$$

for an isothermal system, where $\rho=\rho_0+\delta\rho$ is the fluid mass density with its average ρ_0 and fluctuations $\delta\rho$. The stress tensor $\boldsymbol{\sigma}$ can be expressed as

$$\begin{aligned}\sigma_{\alpha\beta}&=-p\delta_{\alpha\beta}+\sum_{\alpha'\beta'}\eta_{\alpha\beta\alpha'\beta'}\partial_{\beta'}v_{\alpha'}\\&=-p\delta_{\alpha\beta}+\eta_1\partial_\alpha v_\beta+\eta_2\partial_\beta v_\alpha+\eta_3\delta_{\alpha\beta}\sum_\gamma\partial_\gamma v_\gamma,\end{aligned} \tag{12}$$

with the thermodynamic pressure p, the abbreviation $\partial_\alpha v_\beta=\partial v_\beta/\partial r_\alpha$, and $\alpha,\beta,\alpha',\beta',\gamma\in\{x,y,z\}$. Here, we assume a linear dependence of the viscous stress on the velocity gradient [73] and subsequently apply the most general form of an isotropic tensor $\eta_{\alpha\beta\alpha'\beta'}$ [18,30,62]. The viscosity parameters η_1, η_2, and η_3 depend on the particular MPC scheme; we will provide the respective expressions in Sec. IV.

With the stress tensor (12), the Navier-Stokes equation (11) becomes

$$\rho_0\frac{\partial}{\partial t}\boldsymbol{v}=-\nabla p+\eta_2\Delta\boldsymbol{v}+(\eta_1+\eta_3)\nabla(\nabla\cdot\boldsymbol{v}). \tag{13}$$

Note that in the Navier-Stokes equation, only two viscosity parameters appear. However, the equation has to be supplemented by boundary conditions, which in the case of slip or partial slip boundaries include the stress tensor itself [68]. Thus, three viscosity parameters are relevant in general. We can identify η_2 as shear viscosity η, i.e., we set $\eta\equiv\eta_2$, since it appears in front of $\Delta\boldsymbol{v}$. The bulk viscosity η^V is the transport coefficient associated with the dynamic pressure [74]

$$P=-\frac{1}{3}\sum_\alpha\sigma_{\alpha\alpha}=p-\eta^V\nabla\cdot\boldsymbol{v}. \tag{14}$$

By means of Eq. (12), we find

$$\eta^V=(\eta_1+\eta_2+3\eta_3)/3. \tag{15}$$

B. Hydrodynamic correlations

Thermal fluctuations can be included in the Navier-Stokes equations by adding a Gaussian and Markovian stochastic process $\boldsymbol{\sigma}^R$ to the stress tensor $\boldsymbol{\sigma}$ (Landau-Lifshitz Navier-Stokes approach) [18,72,73], with

$$\langle\boldsymbol{\sigma}^R\rangle=\boldsymbol{0}, \tag{16}$$

$$\left\langle\sigma^R_{\alpha\beta}(\boldsymbol{r},t)\sigma^R_{\alpha'\beta'}(\boldsymbol{r}',t')\right\rangle=2k_BT\eta_{\alpha\beta\alpha'\beta'}\delta(\boldsymbol{r}-\boldsymbol{r}')\delta(t-t'). \tag{17}$$

We briefly summarize the theoretical results for velocity autocorrelation functions of an isothermal system, which we will compare to simulations in Sec. V. We refer to Ref. [72] for the derivation of the respective expressions.

First of all, we introduce the Fourier representation of the velocity field for a periodic system via

$$\boldsymbol{v}(\boldsymbol{r},t)=\sum_{\boldsymbol{k}}\boldsymbol{v}(\boldsymbol{k},t)e^{-i\boldsymbol{k}\cdot\boldsymbol{r}}, \tag{18}$$

with $k_\alpha=n_\alpha 2\pi/L_\alpha, n_\alpha\in\mathbb{Z}, \boldsymbol{k}\neq\boldsymbol{0}$. $\boldsymbol{v}(\boldsymbol{k},t)$ can be split into a longitudinal velocity $\boldsymbol{v}^L(\boldsymbol{k},t)=\boldsymbol{k}\boldsymbol{k}^T\boldsymbol{v}(\boldsymbol{k},t)/k^2$ and a transversal velocity $\boldsymbol{v}^T(\boldsymbol{k},t)=(1-\boldsymbol{k}\boldsymbol{k}^T/k^2)\boldsymbol{v}(\boldsymbol{k},t)$. The time dependence of the transversal velocity autocorrelation function (TVACF) is determined by the shear viscosity according to

$$\langle\boldsymbol{v}^T(\boldsymbol{k},t)\cdot\boldsymbol{v}^T(-\boldsymbol{k},0)\rangle=\frac{2k_BT}{\rho_0V}e^{-\nu k^2|t|}, \tag{19}$$

where $\nu=\eta/\rho_0$ is the kinematic viscosity. Sound propagation is determined by the longitudinal velocity autocorrelation function (LVACF), which reads [72]

$$\begin{aligned}&C^L(k,t)\\&=\langle v^L(\boldsymbol{k},t)v^L(-\boldsymbol{k},0)\rangle\\&=\frac{k_BT}{\rho_0V}e^{-\tilde{\nu}k^2|t|/2}\left[\cos(\Omega|t|)+\sqrt{\frac{k^2\tilde{\nu}^2}{4c^2-k^2\tilde{\nu}^2}}\sin(\Omega|t|)\right]\end{aligned} \tag{20}$$

for $4c^2>k^2\tilde{\nu}$. The expression for $4c^2<k^2\tilde{\nu}$ can be found in Ref. [72]. Here, $c=\sqrt{k_BT/m}$ is the isothermal sound velocity, $\Omega=k^2\tilde{\nu}\sqrt{4c^2/(k^2\tilde{\nu}^2)-1/2}$, and $\tilde{\nu}=\tilde{\eta}/\rho_0$, where

$$\tilde{\eta}=(\eta_1+\eta_2+\eta_3) \tag{21}$$

is the viscous contribution to the sound attenuation.

IV. ANALYTICAL CALCULATION OF VISCOSITY PARAMETERS FOR MPC

Since the stress tensor (7) is comprised of the kinetic and collisional parts $\sigma^k_{\alpha\beta}$ and $\sigma^c_{\alpha\beta}$, with a respective continuum representation, we can split the viscosities into kinetic parts η^k_1, η^k_2, and η^k_3, and respective collisional parts η^c_1, η^c_2, and η^c_3.

A. Relations between η_1 and η_2

Evidently, the kinetic stress tensor is symmetric, and therefore $\eta^k_1=\eta^k_2$. For the collisional stress, the symmetry requirement $\sigma^c_{\alpha\beta}=\sigma^c_{\beta\alpha}$ is equivalent to

$$0=\sum_{\alpha\beta}\varepsilon_{\gamma\alpha\beta}\sigma^{i,c}_{\alpha\beta}=\sum_{i\in cell}(\Delta\boldsymbol{p}_i\times\boldsymbol{r}_i)_\gamma=-\sum_{i\in cell}\Delta L_{i\gamma}, \tag{22}$$

where $\varepsilon_{\alpha\beta\gamma}$ is the Levi-Civita tensor. Hence, the collisional stress tensor is only symmetric, i.e., $\eta^c_1=\eta^c_2$, if the angular momentum $\boldsymbol{L}$ is conserved during collisions.

To determine η^c_1 for MPC−a, we consider a fluid in the shear field Eq. (8) for which the stress $\sigma_{\alpha\beta}$ can be easily computed by Eq. (12). The only nonzero off-diagonal elements are

$$\sigma_{xz}=\eta_2\dot{\gamma},\quad \sigma_{zx}=\eta_1\dot{\gamma}. \tag{23}$$

Exploiting the stress tensor (9), we can establish a relation between the stress, shear rate, and the MPC parameters. For the collisional stress, we find

$$\begin{aligned}\left\langle\sigma^{i,c}_{\alpha\beta}\right\rangle&=\frac{-m}{Vh}\sum_i\langle\Delta v_{i\alpha}\Delta r_{i\beta}\rangle=\frac{-m}{Vh}\sum_i\langle\mathcal{C}-1\rangle\langle v_{ic\alpha}\Delta r_{i\beta}\rangle\\&=\frac{m}{Vh}\langle1-\mathcal{C}\rangle\left(1-\frac{1}{N_c}\right)\sum_i\langle v_{i\alpha}\Delta r_{i\beta}\rangle\end{aligned} \tag{24}$$

within the molecular chaos assumption, i.e., we set $\langle v_{j\alpha}\Delta r_{i\beta}\rangle = 0$ for $j \neq i$. Since $\langle v_{iz}\Delta r_{ix}\rangle = 0$ for MPC−a, we directly find $\sigma^c_{zx} = 0$ and hence $\eta^c_1 = 0$ [22]. On the other hand, $\langle v_{ix}\Delta r_{iz}\rangle = \dot\gamma\langle\Delta r^2_{iz}\rangle = \dot\gamma a^2/12 > 0$, which enables us to calculate η^c_2 [66]. The result is equal to that obtained by Green-Kubo relations, which are exploited in Sec. IV B. In summary, we found

$$\eta^k_1 = \eta^k_2, \tag{25}$$

$$\eta^c_1 = \begin{cases} \eta^c_2 & \text{for MPC + a,} \\ 0 & \text{for MPC − a.} \end{cases} \tag{26}$$

B. Green-Kubo relation for shear viscosity

We will focus on MPC−a. Analytical results for the shear viscosity of MPC+a can be found in Ref. [65]. The shear viscosity $\eta \equiv \eta_2$ is obtained by the Green-Kubo relation [74]

$$\eta = \frac{V}{k_BT}\int_0^\infty dt\,\langle\sigma_{xz}(t)\sigma_{xz}(0)\rangle \tag{27}$$

from the stress tensor correlation function. The correlation function $\langle\sigma_{xz}(t)\sigma_{xz}(0)\rangle$ comprises autocorrelation functions of the kinetic and collisional stress tensors, respectively, as well as cross terms $\langle\sigma^k_{xz}\sigma^c_{xz}\rangle$. By simulations, we determine the cross correlations for a wide range of MPC parameters and find $\langle\sigma^{i,k}_{xz}\sigma^{i,c}_{xz}\rangle = 0$ for the particle-level stress tensor of Eq. (7). So far, we have not been able to prove this relation analytically, but we will assume that it holds in the following. As a consequence, the viscosity is simply the sum of a kinetic and collisional contribution. For the kinetic viscosity, we find within the molecular chaos approximation [17,63,64,66,75]

$$\begin{aligned}\eta^k_2 &= \frac{V}{k_BT}\left(\frac{h}{2}\left\langle\left(\sigma^{i,k}_{xz}(0)\right)^2\right\rangle + h\sum_{l=1}^{\infty}\left\langle\sigma^{i,k}_{xz}(lh)\sigma^{i,k}_{xz}(0)\right\rangle\right)\\ &= \frac{Vh}{k_BT}\left\langle\left(\sigma^{i,k}_{xz}(0)\right)^2\right\rangle\left(\frac{1}{2}+\sum_{l=1}^{\infty}f^l\right)\\ &= \frac{Nk_BT}{V}h\left(\frac{1}{1-f}-\frac{1}{2}\right),\end{aligned} \tag{28}$$

where we used $\langle v_{ix}(t+h)v_{iz}(t+h)\rangle_{\mathcal{C}} = f\langle v_{ix}(t)v_{iz}(t)\rangle_{\mathcal{C}}$, and $\langle\cdots\rangle_{\mathcal{C}}$ denotes the average over the collision operator, which we perform before the ensemble average. The factor f reads [17,63,64,66,75]

$$f = \frac{1}{N_c} + \left(1-\frac{1}{N_c}\right)\frac{1}{5}[1+2\cos(\alpha)+2\cos(2\alpha)] \tag{29}$$

for SRD−a and $f = 1/N_c$ for AT−a [17]. Here, and in the following, we do not account for particle number fluctuations in a cell, since their contribution to the viscosity coefficients are negligible for $N_c > 5$.

Similarly, the collisional viscosity of MPC−a follows as [66]

$$\begin{aligned}\eta^c_2 &= \frac{V}{k_BT}\frac{h}{2}\left\langle\sigma^{i,c}_{xz}(0)\sigma^{i,c}_{xz}(0)\right\rangle\\ &= \frac{1}{2k_BTVh}\sum_{i,j}\langle\Delta p_{ix}\Delta p_{jx}\rangle\langle\Delta r_{iz}\Delta r_{jz}\rangle = \frac{Nma^2}{12Vh}g\end{aligned} \tag{30}$$

by assuming that in MPC−a the momentum change $\Delta\boldsymbol{p}_i$ is independent of the position $\Delta\boldsymbol{r}_i$, and by utilizing $\langle\Delta r^2_{iz}\rangle = a^2/12$. Note that we neglect all higher correlations $\langle\sigma^{i,c}_{xz}(lh)\sigma^{i,c}_{xz}(0)\rangle$ for $l = 1,2,3,\ldots$, which is motivated by simulation results. Furthermore, we defined $g = m\sum_{i,\alpha}\langle\Delta v_{i\alpha}\Delta v_{i\alpha}\rangle/(6Nk_BT)$, which becomes

$$g = \frac{2}{3}\left(1-\frac{1}{N_c}\right)(1-\cos\alpha) \tag{31}$$

for SRD−a and $g = 1 - 1/N_c$ for AT−a [17]. In Ref. [75], the same result for the viscosity was derived by calculating the momentum transfer across a plane in shear flow.

A calculation of the collisional viscosity by means of a Green-Kubo relation was also performed in Ref. [69] with a stress tensor defined on the cell rather than the particle level. In that case, the correlations $\langle\sigma^c_{xz}(lh)\sigma^c_{xz}(0)\rangle$ and $\langle\sigma^k_{xz}\sigma^c_{xz}\rangle$ are in fact not negligible [69].

C. Green-Kubo relation for bulk viscosity

In terms of the dynamic pressure P and its fluctuations δP defined as

$$P = -\frac{1}{3}\sum_\alpha\sigma_{\alpha\alpha}, \tag{32}$$

$$\delta P = P - \langle P\rangle - \frac{2}{3V}(E_{\rm kin} - \langle E_{\rm kin}\rangle), \tag{33}$$

the bulk viscosity follows from the Green-Kubo relation [74]

$$\eta^V = \frac{V}{k_BT}\int_0^\infty dt\,\langle\delta P(t)\delta P(0)\rangle. \tag{34}$$

Note that by definition δP is independent of the kinetic stress, which therefore does not contribute to η^V. Furthermore, the dynamic pressure P is not affected by the presence or absence of angular momentum conservation, i.e., by the term $\boldsymbol{\omega}\times\boldsymbol{r}_{ic}$ in the collision rule of MPC+a (5). This evidently follows from the calculation

$$\begin{aligned}\sum_{i=1}^{N_c}\boldsymbol{r}_i\cdot[\boldsymbol{\omega}\times(\boldsymbol{r}_i-\boldsymbol{r}_{\rm c.m.})] &= -\sum_{i=1}^{N_c}\boldsymbol{r}_i\cdot(\boldsymbol{\omega}\times\boldsymbol{r}_{\rm c.m.})\\ &= -N_c\boldsymbol{r}_{\rm c.m.}\cdot(\boldsymbol{\omega}\times\boldsymbol{r}_{\rm c.m.}) = 0.\end{aligned} \tag{35}$$

Hence, the bulk viscosity is identical for MPC+a and MPC−a, which constitutes an important result of the article. In analogy with the derivation of Eq. (30) and within the molecular chaos assumption, we find for MPC−a

$$\begin{aligned}\eta^V &= \frac{V}{k_BT}\frac{h}{2}\langle\delta P(0)\delta P(0)\rangle\\ &= \frac{1}{18k_BTVh}\sum_{i\alpha\beta}\langle\Delta p_{i\alpha}\Delta p_{i\beta}\rangle\langle\Delta r_{i\alpha}\Delta r_{i\beta}\rangle\\ &= \frac{1}{18k_BTVh}\frac{m^2a^2}{12}\sum_{i\alpha}\langle\Delta v_{i\alpha}\Delta v_{i\alpha}\rangle = \frac{1}{3}\eta^c_2.\end{aligned} \tag{36}$$

TABLE I. Viscosity relations for MPC±a variants. $\eta = \eta_2$ is the shear viscosity and $\eta^V = (\eta_1 + \eta_2 + 3\eta_3)/3$ is the bulk viscosity. $\eta_1 + \eta_2 + \eta_3$ is the viscous contribution to the sound attenuation coefficient. Note that the viscosities η^k and η^c are different for MPC−a and MPC+a [17]. However, in any case, the bulk viscosity is given by $\eta^V = \eta^c/3$, where η^c is the collisional viscosity of MPC−a.

$\sigma_{\alpha\beta} = -p\delta_{\alpha\beta} + \eta_1\partial_\alpha v_\beta + \eta_2\partial_\beta v_\alpha + \eta_3\delta_{\alpha\beta}\sum_\gamma \partial_\gamma v_\gamma$			
	η_1	η_2	η_3
MPC−a	η^k	$\eta = \eta^k + \eta^c$	$-2\eta^k/3$
MPC+a	$\eta = \eta^k + \eta^c$	η	$-2\eta/3 + \eta^V$

D. Resulting stress tensor for MPC fluid

1. MPC−a

For MPC−a we established the relations $\eta_1^k = \eta_2^k \equiv \eta^k$, $\eta_1^c = 0$, $0 < \eta_2^c \equiv \eta^c$, and $\eta^V = \eta^c/3$. Using Eqs. (15) and (12), this leads to the stress tensor

$$\sigma_{\alpha\beta} = -p\delta_{\alpha\beta} + \eta^k\left(\partial_\alpha v_\beta + \partial_\beta v_\alpha - \frac{2}{3}\delta_{\alpha\beta}\sum_\gamma \partial_\gamma v_\gamma\right) + \eta^c\partial_\beta v_\alpha. \tag{37}$$

Analytical expressions for η^k and η^c are provided in Eqs. (28) and (30). We like to emphasize that Eq. (37) agrees with the stress tensor derived in Refs. [15,76].

2. MPC+a

For MPC+a we found $\eta_1 = \eta_2 \equiv \eta$, and the stress tensor reads

$$\sigma_{\alpha\beta} = -p\delta_{\alpha\beta} + \eta\left(\partial_\alpha v_\beta + \partial_\beta v_\alpha - \frac{2}{3}\delta_{\alpha\beta}\sum_\gamma \partial_\gamma v_\gamma\right) + \eta^V\delta_{\alpha\beta}\sum_\gamma \partial_\gamma v_\gamma. \tag{38}$$

Here, the bulk viscosity is $\eta^V = \eta^c/3$, where η^c is the collisional viscosity of MPC−a. Note that, in general, the viscosities η^k and η^c are different for MPC−a and MPC+a.

Table I summarizes our findings in terms of the parameters η_1, η_2, and η_3.

V. SIMULATIONS

A. Viscosities η_1 and η_2

To determine η_1 and η_2, we perform shear simulations using Lees-Edwards boundary conditions [70]. The viscosities follow from Eq. (23), with the stress tensor calculated according to Eq. (9). Our simulation results confirm Eqs. (25) and (26) for both SRD±a and AT±a. Moreover, the simulations validate the analytical formula for η^c for AT−a and SRD−a. As in previous simulation studies, we find that the analytical formulas for η^k of MPC−a become increasingly imprecise for smaller time steps due to the applied molecular chaos assumption in their derivation. However, the total shear viscosity agrees very well with the theoretical expression, even at small collision times, because the collisional viscosity dominates at small h [67].

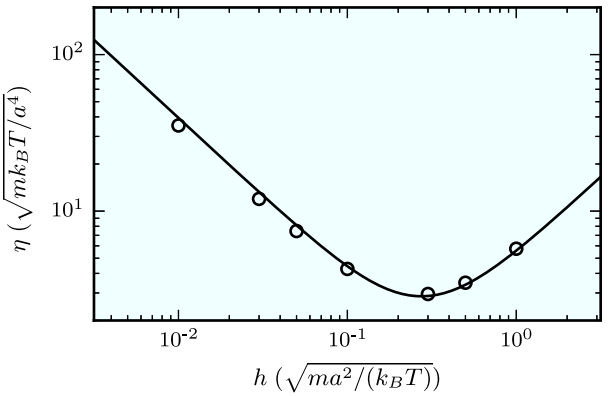

FIG. 1. Shear viscosity η for a SRD+a fluid. The open symbols denote simulation results for the MPC parameters $\langle N_c\rangle = 10$, $\alpha = 130°$, the shear rate $\dot\gamma = 0.01\sqrt{k_BT/(ma^2)}$, and the size of the cubic simulation box $L = 40a$. The solid line represents the theoretical result provided in Ref. [65]. The measured values are also listed in Table II.

The analytical expressions for the shear viscosity of SRD+a and AT+a given in Ref. [65] are found to be less accurate than those for the nonangular-momentum-conserving variants, as indicated in Fig. 1 and Table II.

B. Bulk viscosity

We measure the bulk viscosity by means of the Green-Kubo relation (34) performing equilibrium simulations. The integral is evaluated using the trapezoidal rule to account for the discrete time process. The correlation function $\langle \delta P(t)\delta P(0)\rangle$ decays extremely rapidly. Already after one collision step, the correlation function is essentially zero. Hence, η^V is well described by Eq. (36), with the essential contribution at zero time lag. The measured bulk viscosities are presented in Fig. 2. They agree very well with the analytical prediction.

We also determined the bulk viscosity for two-dimensional MPC fluids and found $\eta^V = \eta^c/2$, in agreement with theoretical calculations similar to those of Sec. IV. Hence, in general, the bulk viscosity is $\eta^V = \eta_c/d$, where d denotes the spatial dimension.

C. Viscous contribution to sound attenuation

To calculate the longitudinal velocity correlation function (20), we perform the Fourier transformation

$$\boldsymbol{v}(\boldsymbol{k},t) = \frac{1}{N}\sum_{i=1}^{N}\boldsymbol{v}_i(t)e^{i\boldsymbol{k}\cdot\boldsymbol{r}_i(t)} \tag{39}$$

of the MPC particle velocities.

TABLE II. Measured and respective theoretical (Ref. [17]) shear viscosities of MPC+a variants.

	$h/\sqrt{ma^2/(k_BT)}$	0.01	0.03	0.1	0.3	1
SRD+a	$\eta/\sqrt{mk_BT/a^4}$	35.2	11.9	4.26	2.94	5.75
	analytical	39.3	13.2	4.44	2.87	5.59
AT+a	$\eta\sqrt{mk_BT/a^4}$	32.0	10.9	4.09	3.21	6.92
	analytical	35.9	12.1	4.23	3.12	6.79

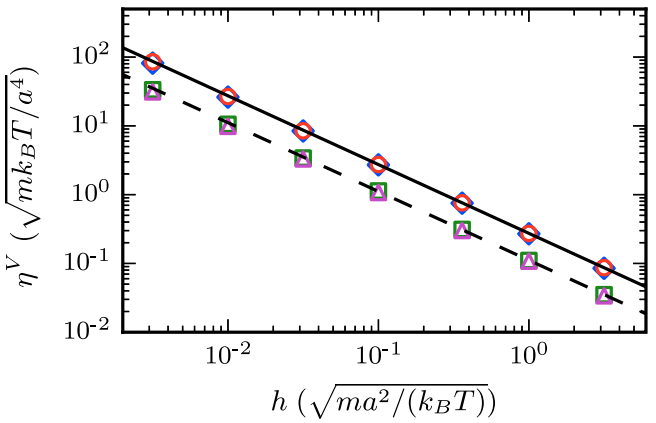

FIG. 2. (Color online) Bulk viscosities of MPC±a variants for various collision steps h. Circles (red) and diamonds (blue) correspond to SRD−a and SRD+a fluids, respectively, while the squares (green) and triangles (magenta) correspond to AT−a and AT+a fluids. The simulation parameters are $\langle N_c\rangle = 10$, $\alpha = 130°$, and $L = 10a$ for SRD, and $\langle N_c\rangle = 5$ for AT. The black lines represent the theoretical expectation $\eta^V = \eta^c/3$, where η^c is the collisional viscosity of MPC−a [Eq. (30)]. The top solid and bottom dashed line correspond to SRD and AT, respectively.

The decay of the correlation function (20) is governed by the viscosity $\tilde{\eta} = \eta_1 + \eta_2 + \eta_3 = \frac{2}{3}(\eta_1 + \eta_2) + \eta^V$. For the non-angular-momentum-conserving variants of MPC, the expression reduces to $\tilde{\eta} = 4\eta^k/3 + \eta^c$, as already discussed in Refs. [11,14,72], which includes the bulk viscosity.

More importantly, the bulk viscosity also contributes to sound attenuation in an angular-momentum-conserving MPC fluid. The effect of η^V is clearly visible for both SRD+a and AT+a in Fig. 3. Since $\eta^c \sim h^{-1}$ and $\eta^k \sim h$, the bulk viscosity contributes significantly to the decay of the longitudinal correlation function at small collision time steps.

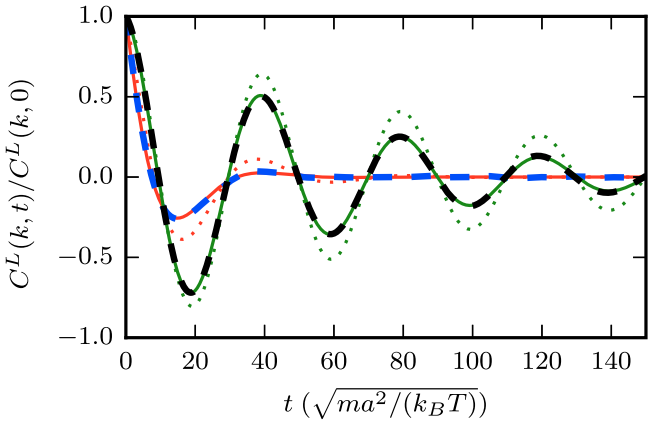

FIG. 3. (Color online) Longitudinal velocity autocorrelation function for $k = 2\pi/L$ and the length $L = 40a$ of a cubic box. The red and blue lines correspond to SRD+a with $\langle N_c\rangle = 10$, $\alpha = 130°$, and $h/\sqrt{ma^2/(k_BT)} = 0.01$; the green and black lines correspond to AT+a with $\langle N_c\rangle = 10$ and $h/\sqrt{ma^2/(k_BT)} = 0.05$. Dashed lines represent simulation results. The solid lines represent the theoretical expression Eq. (20) with $\tilde{\nu} = (4\eta/3 + \eta^V)/\rho_0$, while for the dotted lines the viscosity $\tilde{\nu} = (4\eta/3)/\rho_0$ without bulk contribution is used.

We calculated the LVACF for several collision step sizes and found good agreement with the theoretical prediction as long as the time step h is small, i.e., $h/\sqrt{ma^2/(k_BT)} \lesssim 0.1$. As discussed in Refs. [67,72], larger time steps result in a substantial heat transfer between cells in the streaming step, and consequently the isothermal theory is no longer applicable.

VI. SUMMARY AND CONCLUSIONS

We have determined the viscous transport coefficients for SRD and AT variants of MPC fluids by both analytical considerations and simulations. As a main result, we find a nonzero bulk viscosity for all MPC variants, with and without angular momentum conservation.

A nonzero bulk viscosity for MPC-SRD−a has already been indicated in Ref. [11] in connection with the stress tensor of Ref. [15]. An alternative stress tensor has been formulated, which differs only by a term of vanishing divergence from Eq. (37), and thus it yields the identical Navier-Stokes equations [11,14,72]. However, in Ref. [14], it has been concluded that the bulk viscosity for this stress tensor is zero. The lack of angular momentum conservation leaves more viscosity parameters undetermined than in an angular-momentum-conserving fluid. Hence, by considering the shear viscosity and the sound attenuation factor only, the lack or presence of a bulk viscosity cannot be verified, which renders the various stress tensors seemingly equivalent. However, the Navier-Stokes equations have to be supplemented by boundary conditions, which can depend explicitly on the stress tensor, as is the case with (partial) slip boundary conditions. As a consequence, all three viscosity parameters determine the velocity field, and only the stress tensor Eq. (37) is appropriate for MPC−a fluids [68].

The situation is different for angular-momentum-conserving fluids, where the symmetry requirement of the stress tensor reduces the number of independent viscosity parameters to two. Hence, the shear viscosity and the sound attenuation factor determine η^V uniquely. On the contrary, the bulk viscosity is an integral part of the sound attenuation factor $\tilde{\eta}$. Specifically for MPC at small collision time steps, where the collisional viscosity η^c dominates the shear viscosity and $\eta \approx \eta^c$, the bulk viscosity is essential for the correct sound attenuation factor. We confirmed the strong influence of the bulk viscosity on the decay of the sound correlation function for MPC+a versions by simulations. The presence of η^V has consequences for all those correlation functions, which include the longitudinal mode. In particular, the velocity correlation functions are affected, such as those of colloids.

In addition, our studies confirm that the stress tensor derived in Ref. [15] is appropriate for MPC−a fluids. This has already been evident by previous MPC simulation studies for systems with slip boundary conditions [68].

We found that the shear and bulk viscosity of a MPC fluid are of the same order of magnitude. For many real fluids, such as water, the bulk viscosity is hundreds to thousands of times larger than the shear viscosity [12]. However, the effect of a large bulk viscosity is most pronounced at high-frequency hydrodynamics, where compressibility effects matter most.

The presence of a nonzero bulk viscosity is seemingly in contradiction with the ideal gas equation of state of MPC and the zero bulk viscosity of an ideal gas. As is evident, the bulk viscosity is determined by collisions only. Hence, for a weakly interacting MPC fluid, which we may call a gas, η^c is negligibly small and we may set it to zero. Hence, we reach the ideal gas limit for large collision time steps. This is supported by the Schmidt number, which assumes gaslike values for large collision time steps [77]. Thus, a nonvanishing bulk viscosity is natural for small collision time steps, because here the MPC fluid corresponds to a fluid rather than a gas.

ACKNOWLEDGMENT

We thank Anoop Varghese for helpful discussions.

[1] G. R. McNamara and G. Zanetti, Phys. Rev. Lett. **61**, 2332 (1988).
[2] X. Shan and H. Chen, Phys. Rev. E **47**, 1815 (1993).
[3] B. Dünweg and A. C. Ladd, Adv. Polym. Sci. **221**, 89 (2009).
[4] P. J. Hoogerbrugge and J. M. V. A. Koelman, Europhys. Lett. **19**, 155 (1992).
[5] P. Espanol and P. B. Warren, Europhys. Lett. **30**, 191 (1995).
[6] A. Malevanets and R. Kapral, J. Chem. Phys. **110**, 8605 (1999).
[7] A. Malevanets and R. Kapral, J. Chem. Phys. **112**, 7260 (2000).
[8] R. Kapral, Adv. Chem. Phys. **140**, 89 (2008).
[9] G. Gompper, T. Ihle, D. M. Kroll, and R. G. Winkler, Adv. Polym. Sci. **221**, 1 (2009).
[10] L. Tisza, Phys. Rev. **61**, 531 (1942).
[11] T. Ihle, E. Tüzel, and D. M. Kroll, Phys. Rev. E **72**, 046707 (2005).
[12] M. S. Cramer, Phys. Fluids **24**, 066102 (2012).
[13] T. Ihle and D. M. Kroll, Phys. Rev. E **67**, 066706 (2003).
[14] E. Tüzel, T. Ihle, and D. M. Kroll, Phys. Rev. E **74**, 056702 (2006).
[15] C. M. Pooley and J. M. Yeomans, J. Phys. Chem. B **109**, 6505 (2005).
[16] E. Allahyarov and G. Gompper, Phys. Rev. E **66**, 036702 (2002).
[17] H. Noguchi, N. Kikuchi, and G. Gompper, Europhys. Lett. **78**, 10005 (2007).
[18] M. Theers and R. G. Winkler, Soft Matter **10**, 5894 (2014).
[19] S. H. Lee and R. Kapral, J. Chem. Phys. **121**, 11163 (2004).
[20] M. Hecht, J. Harting, T. Ihle, and H. J. Herrmann, Phys. Rev. E **72**, 011408 (2005).
[21] J. T. Padding and A. A. Louis, Phys. Rev. E **74**, 031402 (2006).
[22] I. O. Götze, H. Noguchi, and G. Gompper, Phys. Rev. E **76**, 046705 (2007).
[23] M. K. Petersen, J. B. Lechman, S. J. Plimpton, G. S. Grest, P. J. in 't Veld, and P. R. Schunk, J. Chem. Phys. **132**, 174106 (2010).
[24] J. K. Whitmer and E. Luijten, J. Phys.: Condens. Matter **22**, 104106 (2010).
[25] T. Franosch, M. Grimm, M. Belushkin, F. M. Mor, G. Foffi, L. Forró, and S. Jeney, Nature (London) **478**, 85 (2011).
[26] M. Belushkin, R. G. Winkler, and G. Foffi, J. Phys. Chem. B **115**, 14263 (2011).
[27] S. Poblete, A. Wysocki, G. Gompper, and R. G. Winkler, Phys. Rev. E **90**, 033314 (2014).
[28] A. Malevanets and J. M. Yeomans, Europhys. Lett. **52**, 231 (2000).
[29] C.-C. Huang, R. G. Winkler, G. Sutmann, and G. Gompper, Macromolecules **43**, 10107 (2010).
[30] C. C. Huang, G. Gompper, and R. G. Winkler, J. Chem. Phys. **138**, 144902 (2013).
[31] A. Lamura, G. Gompper, T. Ihle, and D. M. Kroll, Europhys. Lett. **56**, 319 (2001).
[32] J. T. Padding and A. A. Louis, Phys. Rev. Lett. **93**, 220601 (2004).
[33] A. Wysocki, C. P. Royall, R. G. Winkler, G. Gompper, H. Tanaka, A. van Blaaderen, and H. Löwen, Soft Matter **5**, 1340 (2009).
[34] I. O. Götze and G. Gompper, Europhys. Lett. **92**, 64003 (2010).
[35] S. P. Singh, R. G. Winkler, and G. Gompper, Phys. Rev. Lett. **107**, 158301 (2011).
[36] M. A. Webster and J. M. Yeomans, J. Chem. Phys. **122**, 164903 (2005).
[37] J. F. Ryder and J. M. Yeomans, J. Chem. Phys. **125**, 194906 (2006).
[38] M. Ripoll, R. G. Winkler, and G. Gompper, Phys. Rev. Lett. **96**, 188302 (2006).
[39] L. Cannavacciuolo, R. G. Winkler, and G. Gompper, Europhys. Lett. **83**, 34007 (2008).
[40] S. Frank and R. G. Winkler, Europhys. Lett. **83**, 38004 (2008).
[41] A. Nikoubashman and C. N. Likos, J. Chem. Phys. **133**, 074901 (2010).
[42] D. A. Fedosov, S. P. Singh, A. Chatterji, R. G. Winkler, and G. Gompper, Soft Matter **8**, 4109 (2012).
[43] M.-J. Huang, H.-Y. Chen, and A. Mikhailov, Eur. Phys. J. E **35**, 1 (2012).
[44] R. Chelakkot, R. G. Winkler, and G. Gompper, Phys. Rev. Lett. **109**, 178101 (2012).
[45] L. Jiang, N. Watari, and R. G. Larson, J. Rheol. **57**, 1177 (2013).
[46] H. Noguchi and G. Gompper, Phys. Rev. Lett. **93**, 258102 (2004).
[47] H. Noguchi and G. Gompper, Proc. Natl. Acad. Sci. USA **102**, 14159 (2005).
[48] J. L. Mcwhirter, H. Noguchi, and G. Gompper, Proc. Natl. Acad. Sci. USA **106**, 6039 (2009).
[49] Y.-G. Tao, I. O. Götze, and G. Gompper, J. Chem. Phys. **128**, 144902 (2008).
[50] S. Ji, R. Jiang, R. G. Winkler, and G. Gompper, J. Chem. Phys. **135**, 134116 (2011).
[51] B. Kowalik and R. G. Winkler, J. Chem. Phys. **138**, 104903 (2013).
[52] G. Rückner and R. Kapral, Phys. Rev. Lett. **98**, 150603 (2007).
[53] I. O. Götze and G. Gompper, Phys. Rev. E **82**, 041921 (2010).
[54] M. Yang and M. Ripoll, Phys. Rev. E **84**, 061401 (2011).
[55] J. Elgeti and G. Gompper, Europhys. Lett. **85**, 38002 (2009).
[56] D. J. Earl, C. M. Pooley, J. F. Ryder, I. Bredberg, and J. M. Yeomans, J. Chem. Phys. **126**, 064703 (2007).
[57] J. Elgeti, U. B. Kaupp, and G. Gompper, Biophys. J. **99**, 1018 (2010).

[58] S. Y. Reigh, R. G. Winkler, and G. Gompper, Soft Matter **8**, 4363 (2012).
[59] M. Theers and R. G. Winkler, Phys. Rev. E **88**, 023012 (2013).
[60] T. Ihle, E. Tüzel, and D. M. Kroll, Europhys. Lett. **73**, 664 (2006).
[61] E. Tüzel, G. Pan, T. Ihle, and D. M. Kroll, Europhys. Lett. **80**, 40010 (2007).
[62] G. K. Batchelor, *An Introduction to Fluid Dynamics* (Cambridge University Press, Cambridge, 2000).
[63] T. Ihle and D. M. Kroll, Phys. Rev. E **63**, 020201(R) (2001).
[64] N. Kikuchi, C. M. Pooley, J. F. Ryder, and J. M. Yeomans, J. Chem. Phys. **119**, 6388 (2003).
[65] H. Noguchi and G. Gompper, Phys. Rev. E **78**, 016706 (2008).
[66] R. G. Winkler and C.-C. Huang, J. Chem. Phys. **130**, 074907 (2009).
[67] C.-C. Huang, A. Varghese, G. Gompper, and R. G. Winkler, Phys. Rev. E **91**, 013310 (2015).
[68] M. Yang, M. Theers, J. Hu, G. Gompper, R. G. Winkler, and M. Ripoll (unpublished).
[69] T. Ihle and D. M. Kroll, Phys. Rev. E **67**, 066705 (2003).
[70] M. P. Allen and D. J. Tildesley, *Computer Simulation of Liquids* (Clarendon, Oxford, 1987).
[71] J. H. Irving and J. G. Kirkwood, J. Chem. Phys. **18**, 817 (1950).
[72] C.-C. Huang, G. Gompper, and R. G. Winkler, Phys. Rev. E **86**, 056711 (2012).
[73] L. D. Landau and E. M. Lifshitz, *Fluid Mechanics* (Pergamon, London, 1959).
[74] R. Zwanzig, Annu. Rev. Phys. Chem. **16**, 67 (1965).
[75] E. Tüzel, M. Strauss, T. Ihle, and D. M. Kroll, Phys. Rev. E **68**, 036701 (2003).
[76] T. Ihle, Phys. Chem. Chem. Phys. **11**, 9667 (2009).
[77] M. Ripoll, K. Mussawisade, R. G. Winkler, and G. Gompper, Phys. Rev. E **72**, 016701 (2005).